Available online at www.sciencedirect.com
ScienceDirect
Polymer 48 (2007) 6823–6833
polymer
www.elsevier.com/locate/polymer

Electrospinning of polymer melts: Phenomenological observations

Paul D. Dalton [a,b,*], Dirk Grafahrend [b,c], Kristina Klinkhammer [b,c], Doris Klee [b,c], Martin Möller [b,c]

[a] School of Biological Sciences, University of Southampton, Bassett Cr East, Southampton SO16 7PX, United Kingdom
[b] Deutsches Wollforschungsinstitut, Pauwelsstraße 8, Aachen D 52074, Germany
[c] Department of Textile and Macromolecular Chemistry, RWTH-Aachen, Worringer Weg 1, Aachen D 52074, Germany

Received 6 June 2007; received in revised form 24 September 2007; accepted 24 September 2007
Available online 29 September 2007

Abstract

Melt electrospinning is an alternative to solution electrospinning, however, melt electrospinning has typically resulted in fibers with diameters of tens of microns. In this paper we demonstrate that polypropylene fibers can be reduced from 35 ± 8 μm in diameter, to 840 ± 190 nm with a viscosity-reducing additive. Melt electrospun blends of poly(ethylene glycol)-*block*-poly(ε-caprolactone) (PEG_{47}-*b*-PCL_{95}) and poly(ε-caprolactone) (PCL) produced fibers with micron-scale diameters (2.0 ± 0.3 μm); this was lowered to 270 ± 100 nm by using the gap method of alignment for collection. The collected melt electrospun fibers often fused together where they touched, allowing the stabilization of relatively thick non-woven felts. The melt electrospun collection also included coiled circles and looped patterns of fibers approximately 150–250 μm in diameter. The polymer jet was visible between the collector and spinneret for particularly significant lengths, and underwent coiling and buckling instabilities close to the collector. The focused deposition of melt electrospun fibers was maintained when multiple jets were observed, with the collections from multiple jets separated by 3.8 ± 0.5 mm for a 5 cm collector gap. The frequent fusion points between melt electrospun fibers, and a reduction in diameter for the gap method of alignment, indicated that the melt electrospun fibers are still slightly molten at collection.

Keywords: Scaffold; Tissue engineering; Melt electrospinning

1. Introduction

Electrospinning is a nano- and micro-fiber manufacturing technique that has attracted much recent interest, resulting in hundreds of published articles and reviews [1,2]. It is well-known that both polymer solutions and polymer melts can be electrospun, however, the available literature for melt electrospinning is comparatively limited [3–11]. Electrospinning without solvents (via the melt) may be appealing for applications and configurations where solvent accumulation or toxicity is a concern. Research on melt electrospinning has been restricted so far, likely due to the large fibers reported in the earlier literature [3–5] – up to 50 μm in diameter and typically above 10 μm [3–7,11]. With such large diameter fibers, melt electrospinning provided little advantage over established melt spinning techniques to produce micron-diameter fibers. The benefits of electrospun nanofibers, namely a large surface area to volume ratio (up to 10^3 times of that of a micro-fiber) and mechanical properties (e.g. high bending capacity), require much smaller diameters than those initially described in the melt electrospinning literature. Industrially, advanced textiles and filtration systems are applications where the efficacy of electrospun fibers has been investigated.

However, recent melt electrospinning publications demonstrate that continuous fibers of approximately one micron in diameter are possible, and therefore provide the benefits of nanometer diameter fibers often produced with solution electrospinning [8,10,11]. Melt electrospinning requires cooling

* Corresponding author. Deutsches Wollforschungsinstitut, Pauwelsstraße 8, Aachen D 52074, Germany.
E-mail address: dalton@dwi.rwth-aachen.de (P.D. Dalton).

0032-3861/$ - see front matter © 2007 Elsevier Ltd. All rights reserved.
doi:10.1016/j.polymer.2007.09.037

of the polymeric jet, while solution electrospinning relies on evaporation of the solvent to produce fibers. It is therefore important during solution electrospinning that the evaporated solvent does not accumulate; otherwise, the fiber quality is affected. At the research level, electrospinning experiments performed in enclosed environments are limited – most configurations are in well-ventilated areas [12–15]. In numerous ways, solvent accumulation has dictated the manner in which electrospinning has been researched.

Electrospinning also attracts particular interest in biomedical applications, for the tissue engineering of cell constructs. The sub-micron diameters of electrospun fibers are of similar magnitude to the fibrils often found within extracellular matrix, and initial electrospinning experiments for tissue engineering demonstrate great promise [16–21]. However, since many tissue-engineers wish to combine various cells and electrospun material for clinical use, solvent toxicity is an ongoing concern with solution electrospinning. Volatile (and often toxic) solvents often used for preparing electrospun fibers therefore require removal before contact with cells, or the living body. Such solvent removal can be readily demonstrated where electrospun mats are formed at initial step and then degassed. However, for strategies where the simultaneous deposition of cells and fibers (or fibers deposited directly onto/into the living body) are desirable, the issue of residual solvent (and therefore toxicity) remains. Electrospinning from the polymer melt may allow new approaches to certain aspects of electrospinning, particularly overcoming the technical restrictions governed by solvent accumulation and toxicity.

In this article we highlight the phenomenological observations of melt electrospinning with two different synthetic polymers, and produce sub-micron to micron diameter continuous fibers. We demonstrate a transformation from large-diameter fibers – typical of previous melt electrospinning schemes – to sub-micron diameter fibers with the use of viscosity-reducing additives. One of the polymers, polypropylene, is difficult to dissolve and has therefore been restricted in the solution electrospinning literature. The low melting point block copolymers used in this article have a recent history of biomedical applications, and were previously melt electrospun directly onto cells [8]. The phenomenological observations and descriptions of the process, using a series of different collection systems will contribute to the limited knowledge currently available for melt electrospinning.

2. Experimental

2.1. Materials and copolymer synthesis

All materials and solvents, unless otherwise stated, were purchased from Aldrich Chemicals (Milwaukee, USA). The amphiphilic diblock copolymer PEG_{47}-*block*-PCL_{95} was synthesized by ring opening polymerization, using stannous (II) 2-ethyl hexanoate as a catalyst and mono-methoxy PEG (2000 g/mol) as a macroinitiator and is described elsewhere [22]. The number average block lengths were calculated using ^{1}H NMR. The polymer blends were created by dissolution of PCL (67 000 g/mol) and PEG_{47}-*b*-PCL_{95} into a dichloromethane solution, followed by full removal of the solvent. Commercially available isotatic polypropylene (Novolen 1100 N, melt flow index (MFI): 15 cm^3/10 min [230 °C/2.16 kg]), termed PP-15 for this study, was purchased from Bayer AG (Germany), while the Moplen HP 561 S polypropylene (MFI: 44 cm^3/10 min [230 °C/2.16 kg]), termed PP-44, was acquired from Basell Polyolefine GmbH (Germany). The MFI denotes the volume of polymer that passes through capillary tubing in a set amount of time, and the value is inversely proportional to the viscosity of the polymer. PP-15 has a molecular weight of 210 000 g/mol and polydispersity of 3.5. Similar data for PP-44 was not provided; however, this particular isotactic polymer has a narrow polydispersity and is recommended for extrusion applications. Irgatec CR 76 has been obtained from CIBA (Ciba Specialty Chemicals, Switzerland). The 1.5% blend has been produced using a kneader type 30 EHT with rheometer (Plastograph®/Brabender® GmbH and Co. KG) and kneading at 200 °C for 5 min.

2.2. Electrospinning

The electrospinning collection configurations are schematically drawn in Fig. 1. Unless otherwise indicated, a high negative voltage of 20 kV (Bertran Series 205B, Hicksville, NY) was applied to the spinneret and the fibers collected onto grounded aluminum SEM stubs, covered with a sheet of aluminum foil. The collection distance was 10 cm for the low melting point PCL/PEG-*b*-PCL blends and 4 cm for the high melting point polypropylene. The polymer was pumped to the spinneret with a flow rate between 0.02 and 0.3 mL/h. In the case of the polypropylene, the melt was pumped to

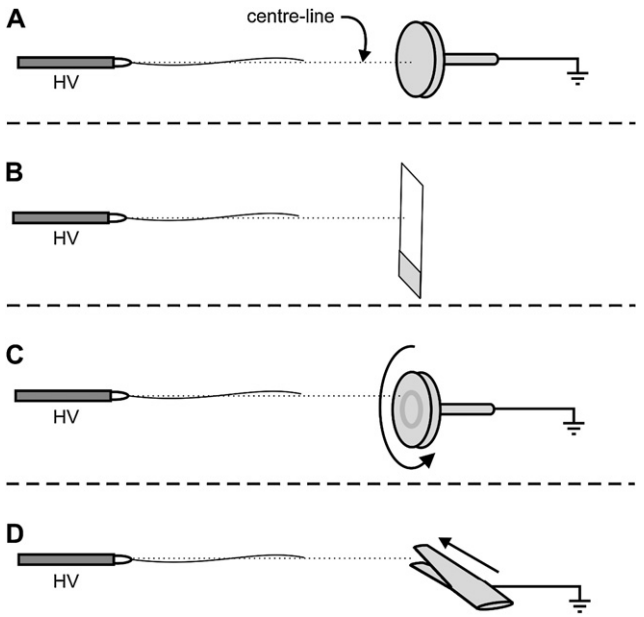

Fig. 1. Schematic of electrospinning collection configurations adopted in this article. (A) A single aluminum SEM stub; (B) a single microscope slide; (C) a single aluminum SEM stub, rotating at 2500 rpm, with the axis of rotation parallel to the centre line; and (D) dual collector with a tapered distance between collectors.

the spinneret with a flow rate of 0.05 mL/h. To prevent poor fiber collection associated with the initial polymer jet, an aluminum foil cover was placed just over the collector, and mechanically withdrawn after the initial 30 s of electrospinning. For the experiments collecting onto SEM stubs, the collection time was 60 s after removal of the conductive cover, while dynamic deposition experiments involved collection of electrospun fibers for only 5 s on a SEM stub rotating at 2500 rpm. Microscope slides were held by hand throughout collection and a voltage of 10 kV used. Stainless steel tweezers (11002-12, Fine Science Tools, Germany) were used as dual collectors and were moved with a syringe pump at a rate of 1 cm/min across the centre line of the polymer jet at a distance of 10 cm from the spinneret. The conditions for solution electrospinning of PCL was performed as previously described [23].

2.3. Heating configurations

The temperatures investigated for melt electrospinning were 90 °C for PEG_{47}-*b*-PCL_{95}/PCL, 270 °C for the polypropylene with a MFI of 44 cm^3/10 min (PP-44), and 320 °C for polypropylene with a MFI of 15 cm^3/10 min (PP-15). Two distinctly different heating configurations were utilized, based upon temperature stability, operator safety, and technical simplicity. The lower temperature heating system adopted the advantages of a highly stable circulatory system to maintain temperature (±0.2 °C) and is schematically shown in Fig. 2. A 1 mL syringe (Injekt, B-Braun) was filled with the polymer powder and heated to the appropriate temperature. Air bubbles were removed by pushing the polymer melt back and forward within the syringe. A flat-tipped stainless 20 G steel spinneret was then attached, and the syringe inserted into the circulator and equilibrated for approximately 20 min at the appropriate temperature. The higher temperature electrospinning system (shown in Fig. 2) contained an electronic controlled heat gun and a second thermometer at the place of the syringe to control the temperature of the melt. The warm air current provided an easy-to-handle and simple heat source, which allowed safe work at high temperatures. Glass syringes with a flat-tipped stainless 20 G steel spinnerets were filled with solid polymer powder and preheated in an electric oven (WTB Binder 115L). Air bubbles were removed as described for the low melting polymers. The syringe was set in the electrospinning system and heated for 25 min, which allowed the system to reach an equilibrium temperature. Electrospinning was performed immediately after removal of the heat gun, in order to minimize the cooling of the syringe and spinneret. Temperatures at the spinneret were determined with a K-type thermocouple.

2.4. Viscosity measurements

A controlled stress rheometer (Rheometric Scientific DSR, USA) measured the viscosity of the polymer melts, at various temperatures and shear rates. The temperatures were reached with an electrically heated cone and plate (4°/25 mm; with a gap of 0.111 mm). The zero-shear viscosity was calculated using creep analysis of the molten polymer. A heat gun aimed at the cone–plate configuration was used in addition to the rheometer heating element to attain 320 °C.

2.5. Scanning electron microscopy (SEM) and light microscopy

The electrospun material on the aluminum SEM stubs were gold-coated and imaged with a Cambridge S360 (Leica, Germany) microscope, or with a Quanta 200 (FEI, United Kingdom). The low-diameter fibers from dual collectors were sampled by passing a copper grid for a transmission electron microscope (TEM) through the suspended fiber collection. The TEM grid was mounted on a SEM stub coated with platinum/gold and imaged in high vacuum mode on the Quanta 200 SEM. An electron beam of 15 kV and a working distance of 7–15 mm were used to image the electrospun material. Fiber diameters were measured using SEM ($n = 30$) and standard deviations used, while representative images of the electrospun fibers are presented. The periodic distance of the perpendicular surface structures on fibers of PP-15 was also measured with SEM ($n = 10$). The microscope slides containing fibers from multiple jets were either imaged on a stereomicroscope (Leica MZ16F, United Kingdom), altering the light to contrast the fibers, or on an inverted light microscope (Zeiss Axio Imager A1, United Kingdom).

3. Results and discussion

The polymers and blends used in this study are summarized in Table 1. The two parameters that significantly affected the

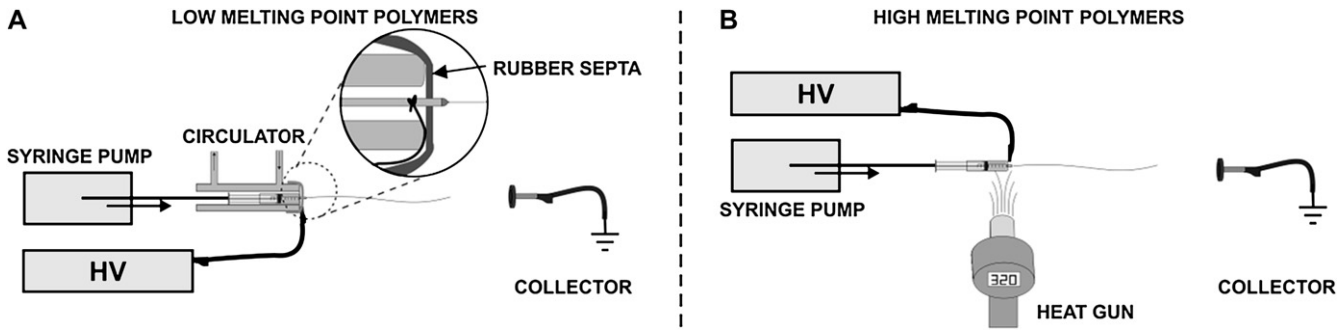

Fig. 2. Schematic of the different heating configurations used for melt electrospinning for (A) low melting point polymers and (B) high melting point polymers.

Table 1
Selected properties and conditions for melt electrospun polymers

Polymer	Electrospinning temperature (°C)	Melting point (°C)	Zero-shear viscosity (Pa s)	Fiber diameter (μm)
PP-44	320	163–167	23	8.6 ± 1.0
PP-15	270	164–166	75	35.6 ± 1.7
PP-15 + 1.5% Irgatec	270	163–165	33	0.84 ± 0.19
PEG_{47}-*block*-PCL_{95} + 30% PCL	90	55–58	49	2.0 ± 0.3
PEG_{47}-*block*-PCL_{95} + 30% PCL (dual collector)	90	55–58	49	0.27 ± 0.10

Viscosity data were measured at the electrospinning temperature.

quality and dimensions of melt electrospun fibers were the viscosity of the polymer melt and the flow rate to the spinneret [8,9]. The viscosity often used for solution electrospinning (0.1–6 Pa s) [24–26] is a magnitude lower than that for these experiments (30–75 Pa s). Conversely, the flow rates for solution electrospinning in literature are a magnitude greater than

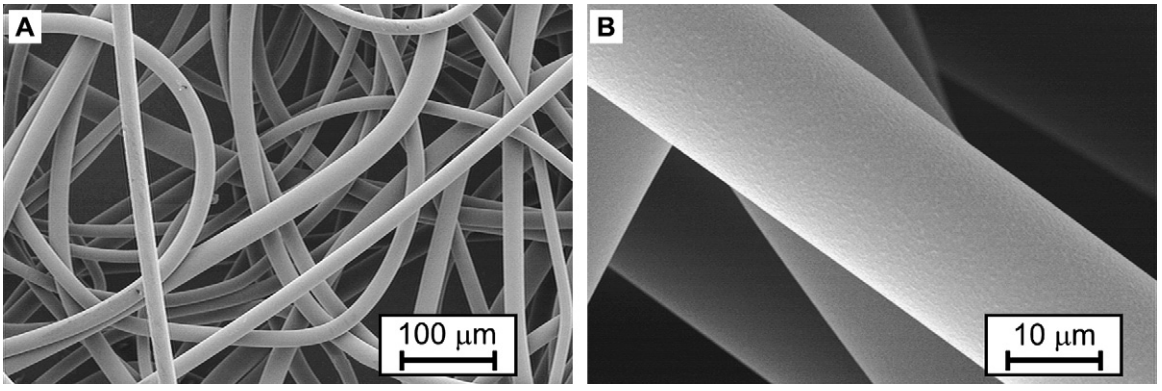

Fig. 3. SEM images of PP-44 fibers that were melt electrospun at 320 °C, with a pump rate of 0.05 mL/h and a collection distance of 4 cm.

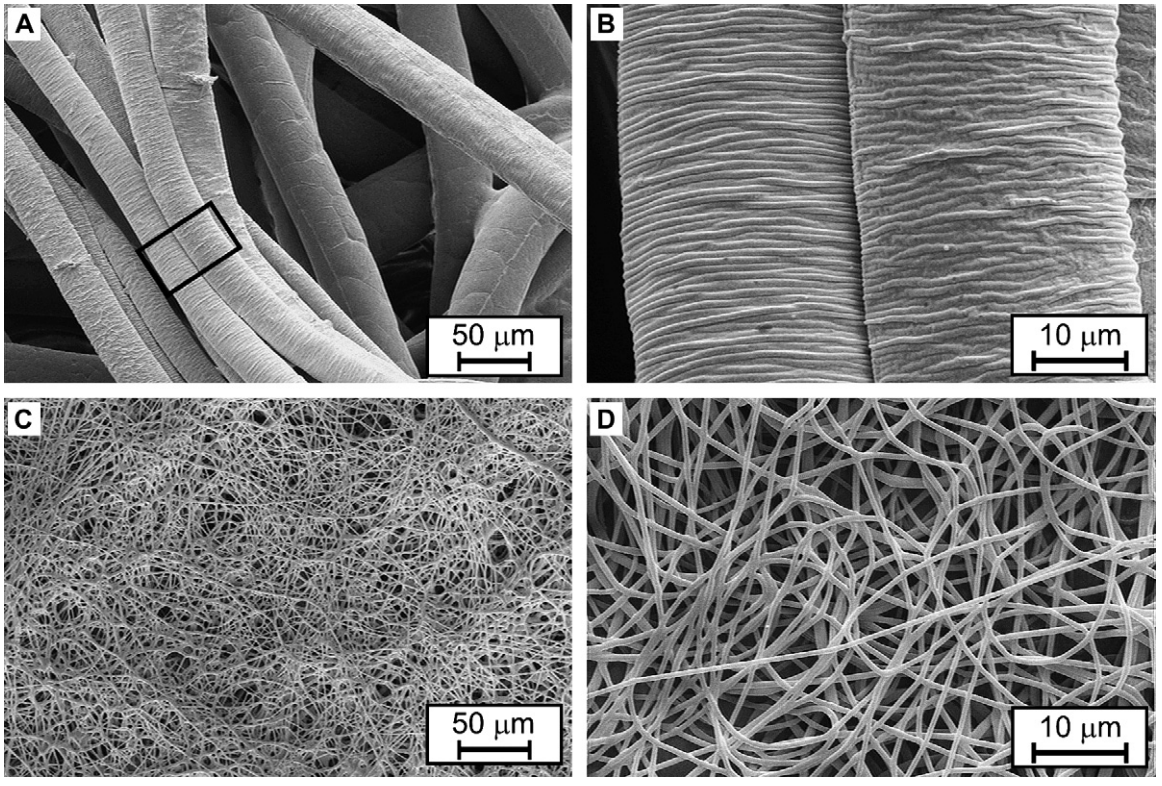

Fig. 4. SEM images of PP-15 fibers without (A and B) and with (C and D) viscosity-reducing additive, melt electrospun at 270 °C, with a pump rate of 0.05 mL/h and a collection distance of 4 cm.

those for melt electrospinning. The low flow rates required for melt electrospinning (0.02–0.05 mL/h) are the disadvantage for industrial applications, but are required since greater charges exist in polymeric liquids with lower flow rates [27]. The highest quality fibers were electrospun from polymer melts with viscosities between 30 and 55 Pa s. The addition of the Irgatec to PP-15 reduced the viscosity from 75 to 33 Pa s.

The four different collection systems used are shown in Fig. 1. A single collector (Fig. 1A) was used for both polypropylene and poly(ethylene glycol)-*block*-poly(ε-caprolactone)/poly(ε-caprolactone) (PEG_{47}-*b*-PCL_{95}/PCL) blends. Melt electrospun PEG_{47}-*b*-PCL_{95}/PCL blends were additionally collected onto a microscope slide (Fig. 1B), a single collector, *with the axis of rotation parallel* to the centre line (Fig. 1C) or onto dual collectors (Fig. 1D).

Two different heating configurations were used for electrospinning the different melting-point polymers, based upon temperature stability, operator safety, and technical simplicity (Fig. 2). For low temperatures (60 °C–90 °C), a circulatory system provided a very constant temperature (±0.2 °C) to the syringe and spinneret, while at higher temperatures

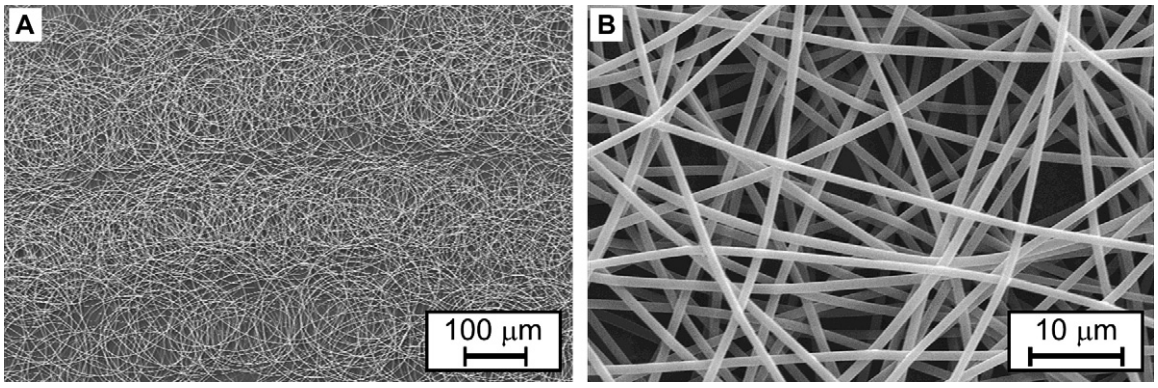

Fig. 5. SEM images of PEG_{47}-*b*-PCL_{95}/PCL electrospun fibers melt electrospun at 90 °C, with a pump rate of 0.05 mL/h and a collection distance of 10 cm.

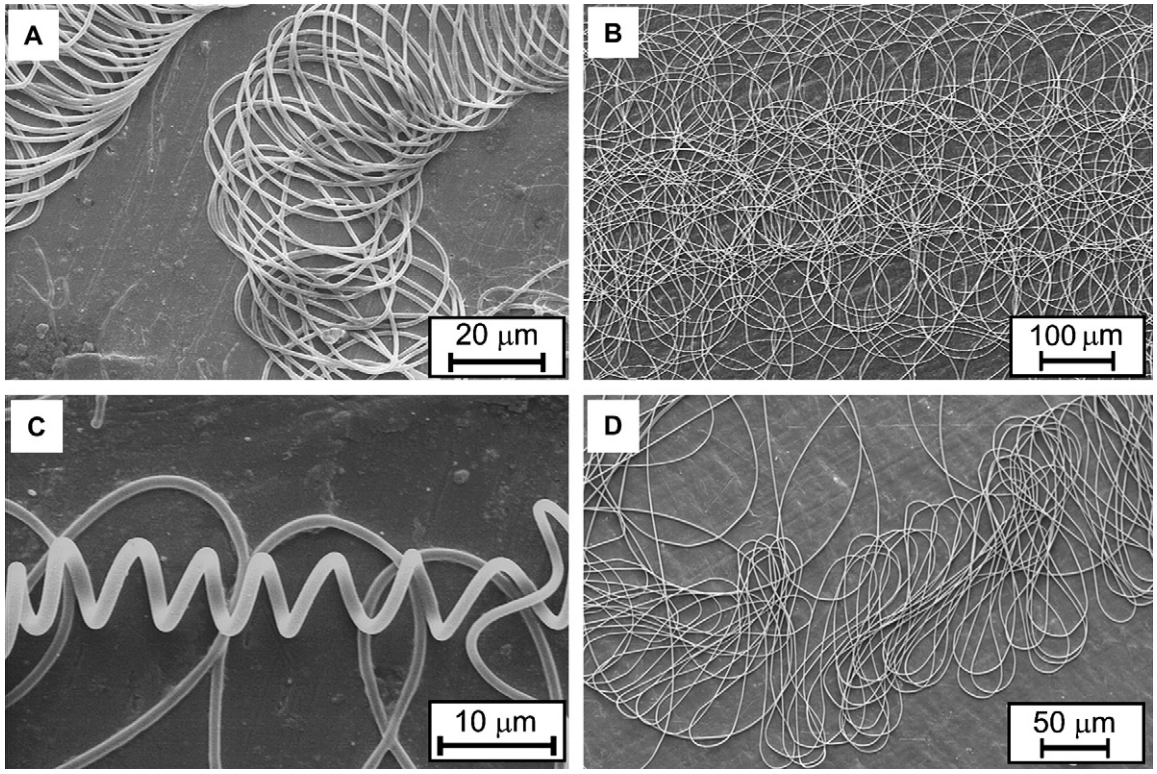

Fig. 6. Examples of commonly observed coiled deposition phenomena for melt electrospun fibers. Circular coils are deposited and can form for (A) PP-15 with Irgatec; or (B) PEG_{47}-*b*-PCL_{95}/PCL. Helical fibers with very short curvature are also periodically seen for (C) PP-15. A different, and very common deposition phenomena, is the looped coils that are elongated as shown for (D) PEG_{47}-*b*-PCL_{95}/PCL blends. Such circular and looped coil depositions are not abnormality, but are consistently observed for melt electrospun samples.

Fig. 7. Photograph of the Taylor cone and polymer jet for melt electrospinning. The molten pendant drop has one single Taylor cone that is relatively elongated, while the jet is particularly long, and is visible for almost the entire distance to the collector. The resulting fibers are solid and 2.0 ± 0.3 μm in diameter.

a flow of heated air melted the polypropylene. A heat gun was technically straightforward, avoided safety issues involving very high temperature circulation systems, and prevented accidental surface contamination of biomaterials with high temperature circulating fluids [28]. A potential issue of overheating and undesirable degradation of the low melting point PEG_{47}-*b*-PCL_{95}/PCL blends [8] is minimized by the circulating heated system.

3.1. Electrospun fiber morphology

Melt electrospinning of unmodified polypropylene (both the PP-44 and PP-15) onto a single collector provided good quality electrospun fibers (Figs. 3 and 4a and b); albeit with a relatively high fiber diameter – this is consistent with earlier observations for melt electrospun material [3–5]. The PP-44 fibers had diameters of 8.6 ± 1.0 μm, and appeared not to fuse with other fibers. Cooling of the polymer jet prior to collection was therefore sufficient, even though the spinneret/collector distance (collection distance) is relatively short (approximately 4 cm). The PP-15 electrospun fibers were 35.6 ± 1.7 μm in diameter but had a very different surface structure from the PP-44 fibers. While melt electrospun PP-44 fibers were smooth and uniform (Fig. 3), PP-15 fibers had a surface structure perpendicular to the direction of the fiber (Fig. 4A and B). Given the large diameter of the fibers, the surface structure is probably a result of extrusion instabilities, or shrinkage due to cooling, with the periodicity of these surface structures on the electrospun fibers being 920 ± 70 nm. The inclusion of viscosity-reducing additive to the PP-15 actively reduces the polymer chain length and therefore viscosity [29,30]. This additive, which is used for melt blowing applications, has a dramatic impact on the diameter of the PP-15 fiber and reduced the diameter from 35.6 ± 1.7 μm to 840 ± 190 nm; however, fusion between the collected fibers was significant (Fig. 4C and D). The surface of these smaller fibers was

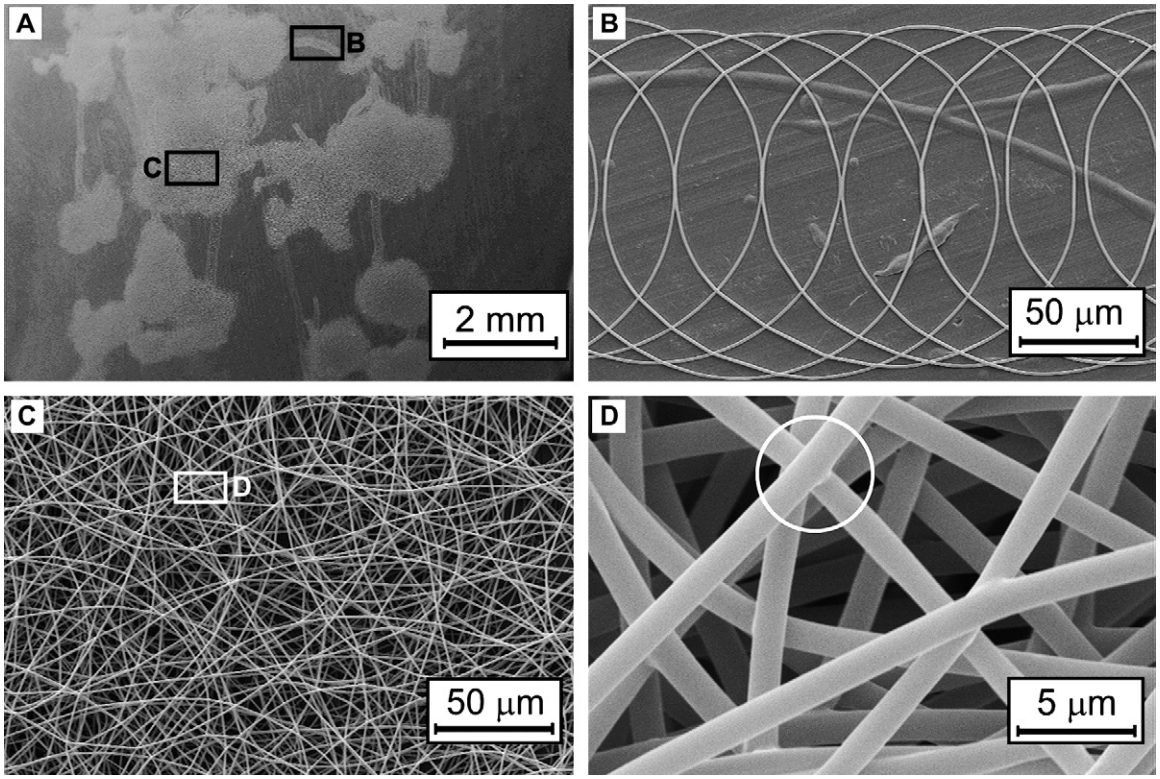

Fig. 8. Deposition phenomena of melt electrospun PEG_{47}-*b*-PCL_{95}/PCL blends. Regional "patches" of electrospun fibers are collected, and the collection is magnified in images B–D. Coiled loops of fibers join some of these regions (B), while the centre of the patches reveals high quality fibers (C) that exhibit some fusion of the fibers (circled in D). These patches were up to one millimeter in height.

smooth, and contrasted with the perpendicularly oriented morphology on the surface of pure PP-15.

The authors' initial experience with melt electrospinning PEG-*b*-PCL diblock copolymers included the fabrication of very poor quality fibers when using the electrospinning parameters (i.e. flow rate, viscosity) commonly adopted for solution electrospinning [9,24–26]. By blending the PEG-*b*-PCL diblock copolymers with a higher molecular weight homopolymer, PCL, we had eliminated poor quality molten fibers from the collected melt electrospun material (Fig. 5). The slight fusion of some high quality fibers within the electrospun mats demonstrate that the electrospun fibers may not fully solidify prior to collection. This is seen in Fig. 5, where the path of the fiber was noticeably altered at the points where the fibers touch, due to contraction of the fiber as it continued to cool on the collector – straight fibers resulted between these fusion points. The diameter of the fibers from PEG_{47}-*b*-PCL_{95}/PCL blends was 2.0 ± 0.3 μm.

Similar to certain solution electrospun systems [31], circular and looped coils were commonly observed with all melt electrospun polymers. These different types of coiled electrospun fibers are shown and described in Fig. 6. The circular and looped fibers in Fig. 6A,B and D, respectively, were particularly common, whilst helical fibers (Fig. 6C) occured only intermittently. Such helical fibers, with small curvature, may form with particularly cooled parts of the polymer jets that have a high surface tension. The tightly coiled deposition (circular and looping) of the electrospun fibers is an interesting phenomenon also seen with solution electrospinning [31].

3.2. Polymer jet formation

When a sufficient voltage is applied, the pendant drop of polymer melt is initially distended and stretched towards the collector. The quality of the electrospun material for the first 30 s is extremely poor, and creates visibly large collected fibers, or "impurities". This portion of the collected material is therefore discarded, and a "sacrificial collector" is used for the first 30 s of collection. Fig. 7 shows a typical photograph of the cone and jet from a polymer melt that result in solid fibers. The visible portion of the jet typically extends for 60–80% of the collection distance, and can be over 10 cm in length when the distance is 15 cm. The Taylor cone was stable for periods up to 10 h, with no visible fluctuations, when flow rates of approximately 0.02–0.05 mL/h were used.

3.3. Deposition phenomena of electrospun fibers

The visible portion of the jet from solution electrospinning typically, but not always, extends for approximately 1 cm from the spinneret before undergoing the instabilities that result in

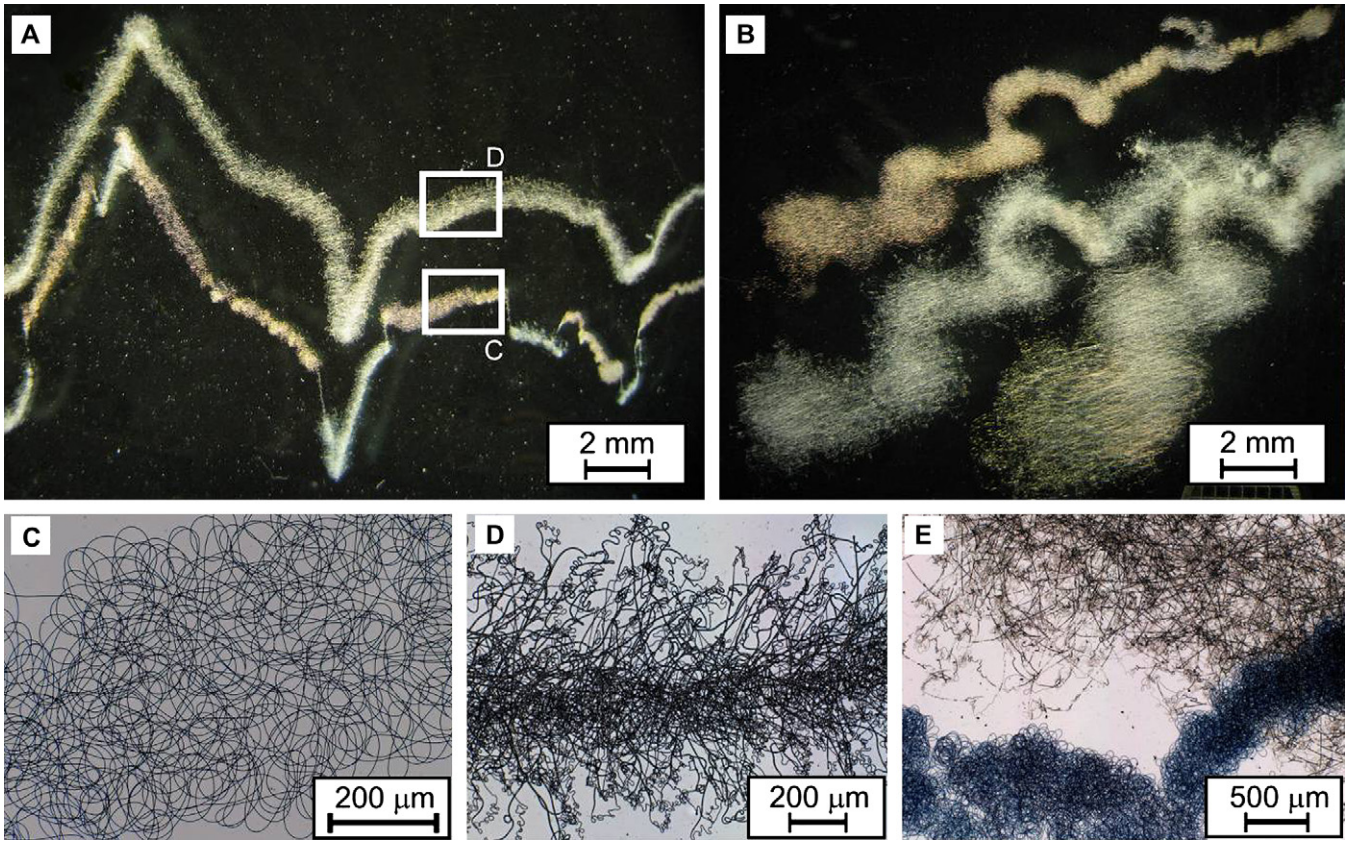

Fig. 9. Photographs of multiple jets from melt electrospun PEG_{47}-*block*-PCL_{95}/PCL blends, collected on a microscope slide showing the collections of (A) two and (B) three jets from a single spinneret. The microscope slide was moved by hand, and fiber deposition paths of different jets are mirrored. The collected material is different from each jet, with high quality fibers (C) collected simultaneously with larger, molten fibers (D). A photograph where the collected material from the two jets crosspaths with each other is shown in (E).

diameter reduction and good quality fiber collection [32,33]. The visible portion of the initial jet for a polymer melt extends much further; estimated to be 10 cm with a collection distance of 15 cm, and results in solid, electrospun fibers as shown in Figs. 5,6 and 8. The molten polymer jet therefore travels the majority of the collection distance before coiling and buckling instabilities occur, and the region of fiber deposition is notably focused. This ''late coiling'' phenomenon has also been recently reported with other melt electrospinning systems [10]. Elongated jets are also reported with electrostatically drawn glycerol, which has a low conductivity compared to commonly used solvents [34].

Fig. 8 shows the deposition of melt electrospun PEG_{47}-*b*-PCL_{95}/PCL blends onto a single collector. ''Patches'' of electrospun fibers contrast with the widely deposited fibers commonly collected during solution electrospinning [12–20,24–26]. While the patches of electrospun fibers indicated a focused deposition, the depositing fiber ''wandered'' across the collector – this was visually seen during collection. In Fig. 8B, a distinctive (circular) coiled loop connects the patches of collected electrospun fibers. Such distinct white ''patches'' of electrospun fibers formed in rapid succession in one area of the collector, before being collected in another region (Fig. 8A). The centre of the patches had high quality electrospun fibers, with depths of up to 1 mm (Fig. 8C). The radius of the coils for PEG_{47}-*b*-PCL_{95}/PCL blends is approximately 75–125 μm. Looped coil deposits were also common (Fig. 6D) structures. The fibers also fused where they touched (Fig. 8D), as previously seen with melt electrospun PEG_{47}-*b*-PCL_{95}/PCL blends (Figs. 5 and 6B). As shown in Fig. 7, the initial visible portion of the jet travels the majority of the collection distance; therefore the reduction of the fiber diameter must occur relatively close to the previously deposited fibers. As the fiber patches attained heights of up to 1 mm the fusion of the electrospun fibers could assist in achieving such relatively thick patches.

While multiple jetting on single, grounded metallic collectors was not observed, it was common for multiple jetting

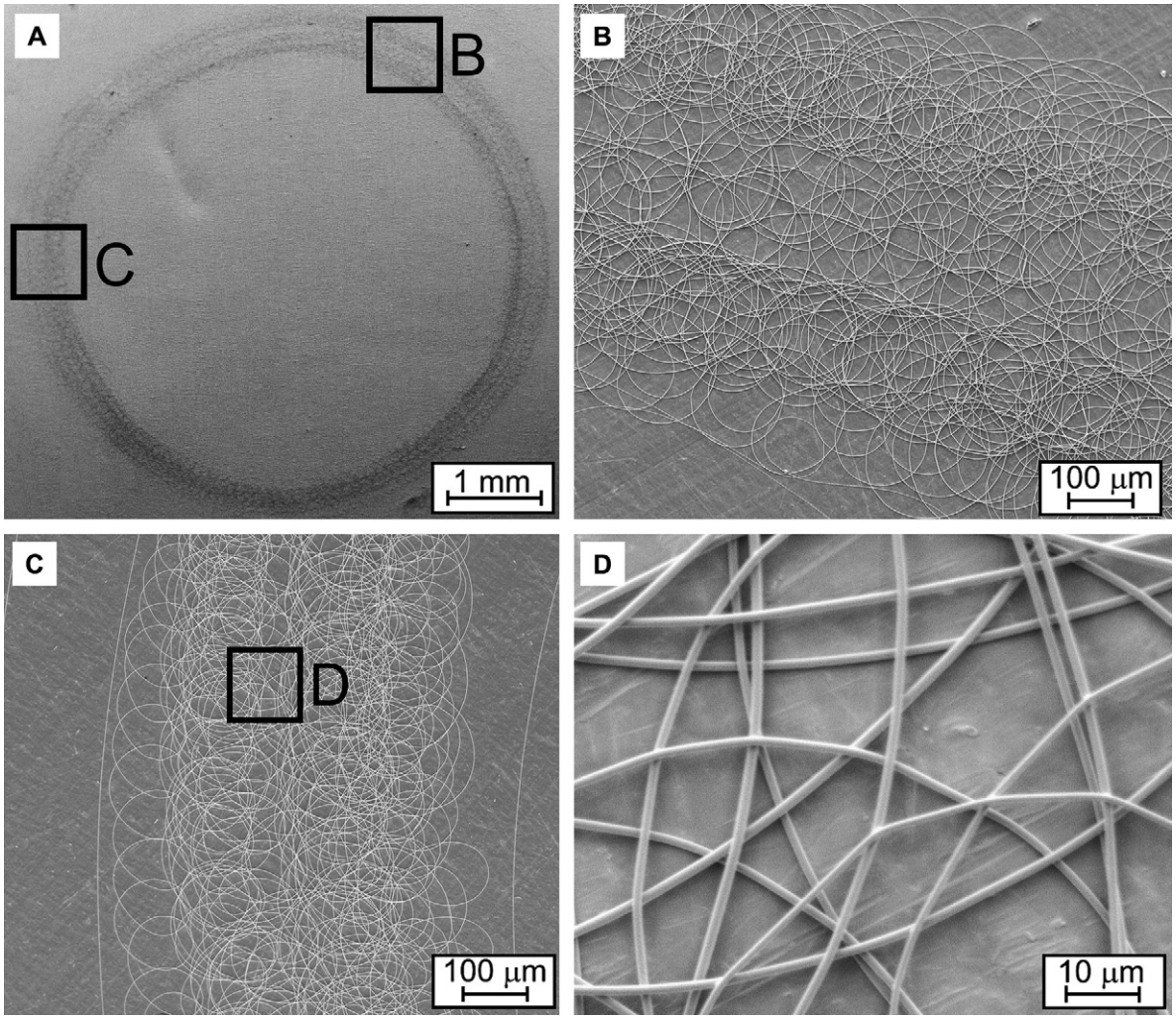

Fig. 10. Deposition of PEG_{47}-*b*-PCL_{95}/PCL electrospun fibers on a collector rotating at 2500 rpm (schematically drawn in Fig. 2C). A ring of electrospun fibers forms due to the focused nature of the deposition (A). The electrospun fibers are coiled (B and C) and the periodicity of the coiling is stretched by the angular rotation (C). There is also some fusion of the electrospun fibers (D).

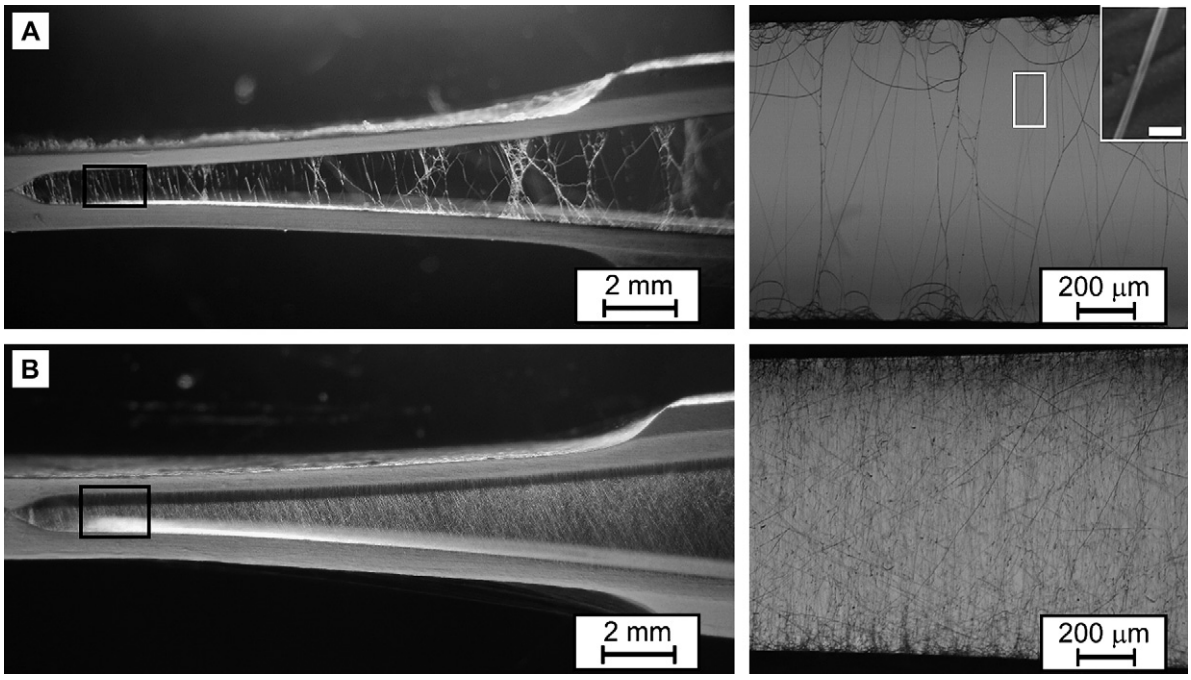

Fig. 11. Images of suspended electrospun fibers on stainless steel tweezers for (A) melt electrospun PEG_{47}-*b*-PCL_{95}/PCL and (B) solution electrospun PCL. The fibers bridge the two metallic parts of the collector, and are covered well with solution electrospun fibers (B). Melt electrospun PEG_{47}-*b*-PCL_{95}/PCL fibers are poor in bridging larger gaps, yet have particularly low diameters of 270 ± 100 nm. The scale bar for inset image is 500 nm.

to occur when microscope slides were used as collectors (Fig. 1B). Simultaneously, multiple fiber jets collect on the glass slide, observed as white, or colored, patches. Moving the microscope slide under centerline demonstrated that the different jet collections mirror the paths of each other, for both double- and triple-jets (Fig. 9A and B). The distance between the collected fibers of two jets was 3.8 ± 0.5 mm for a 50 mm spinneret/collector distance. The fiber quality from the multiple jets, however, was not identical. While one of the collected jets typically had high quality fibers with a small diameter and narrow fiber distribution (Fig. 9C; 2.0 ± 0.3 μm), the second and third jets were of larger diameter and of poorer quality (Fig. 9E; 4.4 ± 2.2 μm). Only one polymer jet was visible during the collection of multiple jets, suggesting splitting of the jet between the spinneret and collector.

To prevent surface charge build-up in a specific region of the collector, we melt electrospun fibers onto a collector rotating around the axis of the jet for 5 s. In this way the place of collection constantly changed. Fig. 10 shows a ring of electrospun fibers with a width of 500 μm with a collection distance of 15 cm. The coiled fiber deposition is stretched by the rotation (2500 rpm) of the collector (Fig. 10B and C). Fig. 10D shows that the collected fibers are again fused together where they are deposited. The deposition is relatively focused – while a similar magnitude of focused deposition can be achieved with solution electrospinning; the collection distance required is only 0.5 mm [35]. Focused deposition may also be achieved with solution electrospinning over similar distances to this study, using concentric rings with intermediate potential applied [36]. In this instance, we achieved similar focused deposition areas as Deitzel et al. [36], without the need for concentric rings.

Dual collectors with solution electrospinning results in oriented fibers, and has been termed the ‘‘gap method of alignment’’ and results in a suspended collection [23,37]. Using moving stainless steel tweezers as the collector (Fig. 1D); the suspended melt electrospun collections could be observed over a range of gaps. It was only when the collector gap narrowed to 1 mm, near the fused portion of the tweezers, that oriented fibers occurred (Fig. 11A), while extremely poor suspended collections resulted at larger gaps. No melt electrospun fiber suspensions formed when the collector gap was greater than 10 mm. This distance is a magnitude lower than solution electrospun PCL, where collector gaps of up to 10 cm result in suspended, oriented, electrospun fibers [23]. Indeed, the entire tweezers were engulfed with solution electrospun PCL fibers (Fig. 11B). Melt electrospinning was therefore poor at generating oriented fiber suspensions between collectors over significant gaps, probably due to the focused nature of deposition, and elongated jet. The melt electrospun PEG_{47}-*b*-PCL_{95}/PCL fibers produced with such dual collectors (Fig. 11A) had very small diameters of 270 ± 100 nm.

Such a significant fiber diameter reduction, by using a dual collection system is an interesting observation that warrants further discussion. Solution electrospun fibers do not have decreased diameters when dual collectors are used [23]. Further investigations into the dual collectors showed that the fibers on each of the two collectors are of larger diameter (c.a. 2 μm), and it is only the suspended fibers with reduced diameters. As previously observed, the

melt electrospun PEG_{47}-*b*-PCL_{95}/PCL fibers were not fully cooled at the time of collection, as seen with the fusion between collected fibers. In combination with the coiling and buckling associated with electrospinning [31], it is proposed that the fibers are mechanically drawn across the collector gap by the coiling action of deposition. Such mechanical drawing of fibers during collection is a phenomenon that melt electrospinning can use to generate even smaller diameter electrospun fibers.

4. Conclusion

Micron and sub-micron melt electrospun fibers were collected with two different synthetic polymers, while oriented melt electrospun fibers were 270 ± 100 nm diameter, which is currently the lowest diameter reported for melt electrospun fibers. As shown with polypropylene, the fiber diameter can be adjusted with viscosity-reducing additives and more than a magnitude reduction in diameter is possible. In addition, the focused fiber deposition allows specific placing and predictable patterning of the electrospun fiber. As cooling is the mechanism for fiber jet solidification (as compared to solvent evaporation), extending the melt electrospinning to multiple spinnerets may compensate for the low flow rates required for high quality fibers. The phenomenological observations exhibited by melt electrospinning warrant further investigations into the modeling and mechanisms of the process.

Acknowledgments

The authors are grateful to Professor Helmut Keul for polymer synthesis; Steven Rutten and Dr. Anton Page for technical assistance with the SEM. The Alexander von Humboldt Foundation is gratefully thanked for its support to PD, while funding from DFG-GRK 1035 'Biointerface'' to support this research is appreciated. The authors thank Dechema e.V. for financial support of the research project (AiF-No. 14263N) from Bundesministerium für Wirtschaft und Technologie (BMWi) via a grant of Arbeitsgemeinschaft industrieller Forschungsvereinigungen ''Otto von Guericke'' e.V./AiF).

References

[1] Ramakrishna S, Fujihara K, Teo W-E, Lim TC, Ma Z. An introduction to electrospinning and nanofibers. Singapore: World Scientific Publishing; 2005.
[2] Pham QP, Sharma U, Mikos AG. Electrospinning of polymeric nanofibers for tissue engineering applications: a review. Tissue Eng 2006;12: 1197–211.
[3] Larrondo L, Manley St JR. Electrostatic spinning from fiber melts. I. Experimental observations on fiber formation and properties. J Polym Sci Polym Phys Ed 1981;19:909–20.
[4] Larrondo L, Manley St JR. Electrostatic spinning from fiber melts. II. Examination of the flow field in an electrically driven jet. J Polym Sci Polym Phys Ed 1981;19:921–32.
[5] Larrondo L, Manley St JR. Electrostatic spinning from fiber melts. III. Electrostatic deformation of a pendant drop of a polymer melt. J Polym Sci Polym Phys Ed 1981;19:933–40.
[6] Kim JS, Lee DS. Thermal properties of electrospun polyesters. Polym J 2000;32:616–8.
[7] Lyons J, Li C, Ko F. Melt electrospinning part I: processing parameters and geometric properties. Polymer 2004;45:7597.
[8] Dalton PD, Klinkhammer K, Salber J, Klee D, Möller M. Direct in vitro electrospinning with polymer melts. Biomacromolecules 2006;7: 686–90.
[9] Dalton PD, Lleixa Calvet J, Mourran A, Klee D, Möller M. Melt electrospinning of poly(ethylene glycol-*block*-ε-caprolactone). Biotechnol J 2006;1:998–1006.
[10] Zhou H, Green TB, Joo YL. The thermal effects on electrospinning polylactic acid melts. Polymer 2007;47:7497–505.
[11] Lee S, Obendorf SK. Developing protective textile materials as barriers to liquid penetration using melt electrospinning. J Appl Polym Sci 2006;102:3430–7.
[12] Lin T, Wang H, Wang X. Self-crimping bicomponent nanofibers electrospun from polyacrylonitrile and elastomeric polyurethane. Adv Mater 2005;17:2699–703.
[13] Yu JH, Fridrikh SV, Rutledge GC. Production of submicrometer diameter fibers by two-fluid electrospinning. Adv Mater 2004;16: 1562–6.
[14] Kim H-W, Kim H-E, Knowles JC. Production and potential of bioactive glass nanofibers as a next generation biomaterial. Adv Funct Mater 2006;16:1529–35.
[15] Zhu Y, Zhang J, Zheng Y, Huang Z, Feng L, Jiang L. Stable, superhydrophobic, and conductive polyanaline/polystyrene. Adv Funct Mater 2006;16:568–74.
[16] Kim H-W, Song J-H, Kim H-E. Nanofiber generation of gelatin-hydroxyapatite biomimetics for guided tissue regeneration. Adv Funct Mater 2005;15:1988–94.
[17] Ma Z, Kotaki M, Inai R, Ramakrishna S. Potential of nanofiber matrix as tissue-engineering scaffolds. Tissue Eng 2005;11:101–9.
[18] Matthews JA, Wnek GE, Simpson DG, Bowlin GL. Electrospinning of collagen nanofibers. Biomacromolecules 2002;3:232–8.
[19] Wang YZ, Blasioli DJ, Kim HJ, Kim HS, Kaplan DL. Cartilage tissue engineering with silk scaffolds and human articular chondrocytes. Biomaterials 2006;27:4434–42.
[20] Shin M, Ishii O, Sueda T, Vacanti JP. Contractile cardiac grafts using a novel nanofibrous mesh. Biomaterials 2004;25:3717–23.
[21] Stankus JJ, Guan J, Fujimoto K, Wagner WR. Microintegrating smooth muscle cells into a biodegradable, elastomeric fiber matrix. Biomaterials 2006;27:735.
[22] Bogdanov B, Vidts A, Van Den Bulcke A, Verbeeck R, Schacht E. Synthesis and thermal properties of poly(ethylene glycol)-poly(epsilon-caprolactone) copolymers. Polymer 1998;39:1631.
[23] Dalton PD, Klee D, Möller M. Electrospinning with dual ring collectors. Polymer 2005;46:611–4.
[24] Min B-M, Lee G, Kim SH, Nam YS, Lee TS, Park WH. Electrospinning of silk fibroin nanofibers and its effect on the adhesion and spreading of normal human keratinocytes and fibroblasts in vitro. Biomaterials 2004;25:1289–97.
[25] Bhattarai N, Edmonson D, Veiseh O, Matsen FA, Zhang M. Electrospun chitosan-based nanofibers and their cellular compatibility. Biomaterials 2005;26:6176–84.
[26] Choi JS, Lee SW, Jeong L, Bae S-H, Min BC, Youk JH, et al. Effect of organosoluble salts on the nanofibrous structure of electrospun poly(3-hydroxybutyrate-*co*-3-hydroxyvalerate). Int J Biol Macromol 2004;34:249–56.
[27] Fridrikh SV, Yu JH, Brenner MP, Rutledge GC. Controlling the fiber diameter during electrospinning. Phys Rev Lett 2003;90. Art No. 144502.
[28] Ohtsu N, Ashino T, Asami K. Silicon contamination adsorbed on pure titanium plate during soaking test in Hanks' balanced saline solution. Mater Trans 2004;45:550–3.
[29] Roth M, Pfaendner R, Simon D. Molecular weight modification of thermoplastic polymers. U.S. Pat. 6,949,594; 2005.
[30] Gande M, Shields P, Roth M, Leukel J, Muller D, Pauquet JR. Peroxide-free vis-breaking additive for improved qualities in meltblown fabrics. In:

International nonwovens technical conference. Conference Proceedings, St. Louis, MO, United States; 2005.
[31] Han T, Reneker DH, Yarin AL. Buckling of jets in electrospinning. Polymer 2007;48(20):6064–76.
[32] Reneker DH, Yarin AL, Fong H, Koombhongse S. Bending instability of electrically charged liquid jets of polymer solutions in electrospinning. J Appl Phys 2000;87:4531–47.
[33] Theron SA, Yarin E, Zussman E, Kroll E. Multiple jets in electrospinning: experiment and modeling. Polymer 2005;46:2889–99.
[34] Shin YM, Hohman MM, Brenner MP, Rutledge GC. Experimental characterization of electrospinning: the electrically forced jet and instabilities. Polymer 2001;42:9955–67.
[35] Sun D, Chang C, Li S, Lin L. Near-field electrospinning. Nano Lett 2006;6:839–42.
[36] Deitzel JM, Kleinmeyer JD, Hirvonen JK, Tan NCB. Controlled deposition of electrospun poly(ethylene oxide) fibers. Polymer 2001;42:8163–70.
[37] Dzenis Y. Spinning continuous fibers for nanotechnology. Science 2004;304:1917–9.